Loss of function mutation in *LOX* causes thoracic aortic aneurysm and dissection in humans

Vivian S. Lee[a], Carmen M. Halabi[a,b], Erin P. Hoffman[c,1], Nikkola Carmichael[c,d], Ignaty Leshchiner[c,d], Christine G. Lian[d,e], Andrew J. Bierhals[f], Dana Vuzman[c,d], Brigham Genomic Medicine[2], Robert P. Mecham[a], Natasha Y. Frank[c,d,g,3], and Nathan O. Stitziel[h,i,j,3]

[a]Department of Cell Biology and Physiology, Washington University School of Medicine, St. Louis, MO 63110; [b]Division of Nephrology, Department of Pediatrics, Washington University School of Medicine, St. Louis, MO 63110; [c]Department of Medicine, Division of Genetics, Brigham and Women's Hospital, Boston, MA 02115; [d]Harvard Medical School, Boston, MA 02115; [e]Department of Pathology, Brigham and Women's Hospital, Boston, MA 02115; [f]Mallinckrodt Institute of Radiology, Washington University School of Medicine, St. Louis, MO 63110; [g]VA Boston Healthcare System, Boston, MA 02132; [h]Cardiovascular Division, Department of Medicine, Washington University School of Medicine, St. Louis, MO 63110; [i]Department of Genetics, Washington University School of Medicine, St. Louis, MO 63110; and [j]McDonnell Genome Institute, Washington University School of Medicine, St. Louis, MO 63110

Edited by J. G. Seidman, Harvard Medical School, Boston, MA, and approved June 7, 2016 (received for review January 27, 2016)

Thoracic aortic aneurysms and dissections (TAAD) represent a substantial cause of morbidity and mortality worldwide. Many individuals presenting with an inherited form of TAAD do not have causal mutations in the set of genes known to underlie disease. Using whole-genome sequencing in two first cousins with TAAD, we identified a missense mutation in the lysyl oxidase (*LOX*) gene (c.893T > G encoding p.Met298Arg) that cosegregated with disease in the family. Using clustered regularly interspaced short palindromic repeats (CRISPR)/clustered regularly interspaced short palindromic repeats-associated protein-9 nuclease (Cas9) genome engineering tools, we introduced the human mutation into the homologous position in the mouse genome, creating mice that were heterozygous and homozygous for the human allele. Mutant mice that were heterozygous for the human allele displayed disorganized ultrastructural properties of the aortic wall characterized by fragmented elastic lamellae, whereas mice homozygous for the human allele died shortly after parturition from ascending aortic aneurysm and spontaneous hemorrhage. These data suggest that a missense mutation in *LOX* is associated with aortic disease in humans, likely through insufficient cross-linking of elastin and collagen in the aortic wall. Mutation carriers may be predisposed to vascular diseases because of weakened vessel walls under stress conditions. *LOX* sequencing for clinical TAAD may identify additional mutation carriers in the future. Additional studies using our mouse model of *LOX*-associated TAAD have the potential to clarify the mechanism of disease and identify novel therapeutics specific to this genetic cause.

whole-genome sequencing | CRISPR/Cas9 | aortic dissection | genetics | lysyl oxidase

Thoracic aortic aneurysms and dissections (TAAD) comprise a large group of heterogeneous conditions with substantial phenotypic diversity. Individuals presenting with an inherited form of TAAD may have evidence of a defined genetic syndrome (e.g., Marfan syndrome, Loeys–Dietz syndrome, Ehlers–Danlos syndrome type IV, or a TGF-β–related vasculopathy) or simply, a family history of TAAD [termed familial thoracic aortic aneurysms and dissections (FTAAD)]. Anatomically, FTAAD can affect various segments of the arterial system from the aortic root and ascending aorta to more distal arterial segments, such as the hepatic or pulmonary arteries. In addition, FTAAD is characterized by significant locus heterogeneity with mutations in a diverse group of genes reported to date (1–10). Despite significant progress in defining the genetic basis of FTAAD, the molecular etiology of many cases remains enigmatic.

Elastin and collagen are two of the major structural components that comprise the arterial wall. Lysyl oxidase (LOX) and its related gene family members are a group of copper-dependent oxidodeaminases that cross-link lysyl residues on these structural proteins in the process of forming proper elastic lamellae and collagen fibers (11). The homozygous knockout (KO) of the murine *Lox* gene results in perinatal death from aortic aneurysm and spontaneous dissection, and mutant *Lox* null mice exhibit highly abnormal aortic histology characterized by fragmented elastic fibers and aberrant smooth muscle cell layers (12, 13). These mouse model findings strongly support the functional significance of LOX in the maintenance of normal arterial wall integrity.

Here, we report a *LOX* missense mutation discovered through whole-genome sequencing in a family with autosomal dominant TAAD, where prior clinical genetic testing was unrevealing. Using genome engineering techniques, we created a mouse model of the specific human mutation to study its in vivo effects. In the heterozygous state, we found that mice with the human mutation displayed abnormal aortas with disorganized assembly of elastic lamellae in the aortic wall, whereas mice homozygous for the human mutation died from perineonatal aortic aneurysm and spontaneous hemorrhage. Together, our data identify another genetic etiology for autosomal dominant TAAD with important implications for clinical patient care.

Significance

The mechanical integrity of the arterial wall is dependent on a properly structured ECM. Elastin and collagen are key structural components of the ECM, contributing to the stability and elasticity of normal arteries. Lysyl oxidase (LOX) normally cross-links collagen and elastin molecules in the process of forming proper collagen fibers and elastic lamellae. Here, using whole-genome sequencing in humans and genome engineering in mice, we show that a missense mutation in *LOX* causes aortic aneurysm and dissection because of insufficient elastin and collagen cross-linking in the aortic wall. These findings confirm mutations in *LOX* as a cause of aortic disease in humans and identify LOX as a diagnostic and potentially therapeutic target.

Author contributions: V.S.L., R.P.M., N.Y.F., and N.O.S. designed research; V.S.L., C.M.H., and N.O.S. performed research; E.P.H., N.C., C.G.L., D.V., B.G.M.P., R.P.M., and N.Y.F. contributed new reagents/analytic tools; V.S.L., C.M.H., I.L., A.J.B., R.P.M., and N.O.S. analyzed data; and V.S.L., R.P.M., N.Y.F., and N.O.S. wrote the paper.

Conflict of interest statement: N.O.S. reports research support from AstraZenica and has served as a consultant to Aegerion Pharmaceuticals, both outside of the scope of this work. The other authors have no disclosures to report.

This article is a PNAS Direct Submission.

[1]Present address: Department of Oncology, Littleton Adventist Hospital, Littleton, CO 80122.

[2]A complete list of individuals from the Brigham Genomic Medicine can be found in *Supporting Information*.

[3]To whom correspondence may be addressed. Email: nfrank@partners.org or nstitziel@wustl.edu.

This article contains supporting information online at www.pnas.org/lookup/suppl/doi:10.1073/pnas.1601442113/-/DCSupplemental.

Results

Characterization of a Family with FTAAD. The proband (Fig. 1*A*, individual III-1) presented to Brigham Genomic Medicine as a 35-y-old Caucasian male for evaluation of his personal and family history of TAAD. His history included a surgical repair of pectus excavatum at two years of age and the diagnosis of a large ascending aortic aneurysm at 19 years old. The aneurysm, which did not involve the aortic root and extended to the brachiocephalic artery, measured 10.5 cm in diameter and was discovered on chest computed tomography imaging as part of an evaluation for complaints of chest pain and cough. The patient underwent a valve-sparing aortic root replacement. The histopathological analysis of his resected aortic tissue found a contained posterior rupture with evidence of cystic medial necrosis and fragmented external elastic lamella. Based on his medical history and suggestive physical features (which included tall stature, high arched palate, and dental crowding), he was given a clinical diagnosis of Marfan syndrome. However, genetic testing, which included fibrillin-1 (*FBN1*) gene sequencing and multiplex ligation-dependent probe amplification, transforming growth factor beta receptor 1 (*TGFBR1*) gene sequencing, and transforming growth factor beta receptor 2 (*TGFBR2*) gene sequencing, was negative.

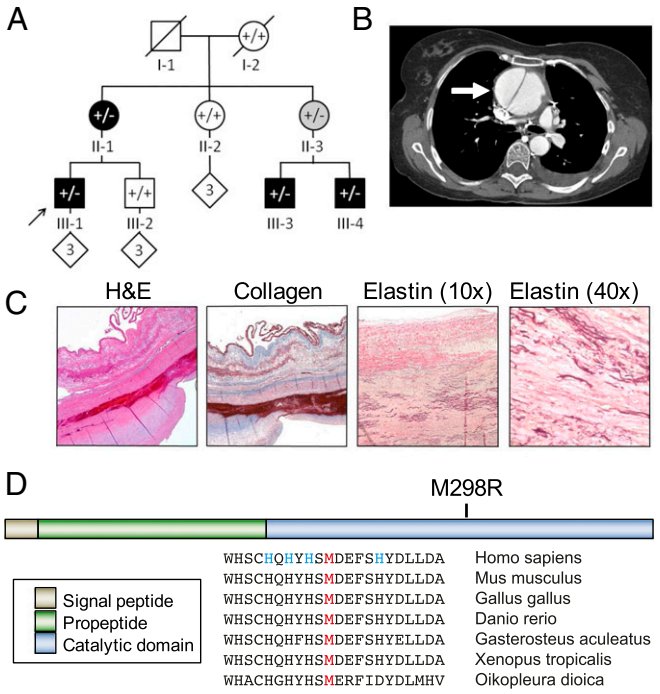

Fig. 1. FTAAD associated with *LOX* mutation. (*A*) The family's pedigree shows autosomal dominant inheritance of FTAAD. Black symbols indicate affected individuals with arterial dissection or aneurysm. Gray symbols indicate individuals affected with arterial tortuosity. White symbols indicate unaffected individuals; – indicates presence of the mutation. (*B*) Contrast-enhanced axial computed tomography image from individual II-1 showing ascending aortic aneurysm (arrow) with dissection and an intimal flap separating the false and true lumens. (*C*) Histologic evaluation of aortic tissue resected from individual II-1. H&E staining shows abnormal architecture and a dissection tear. Masson's trichrome staining for collagen (blue) reveals disorganization of the collagen fibers and disruption of the medial architecture. Verhoeff–van Gieson staining for elastin (dark-purple fibers) illustrates disarray and fragmentation of elastic fibers. (*D*) The location of the M298R missense mutation is depicted in relation to the domains of the LOX protein. Methionine at position 298 is highly conserved as shown by the homologous protein sequences from multiple organisms shown below. Histidine positions that are essential for copper binding and/or LOX catalytic activity (14) are highlighted in blue.

His physical examination was notable for pectus excavatum, presence of venous varicosities in his right lower extremity, positive thumb but not wrist signs, and skin striae on his flanks. A review of his family history suggested an autosomal dominant disorder (Fig. 1*A*).

The mother of the proband (Fig. 1*A*, individual II-1) was also evaluated in our clinic because of her history of acute ascending aortic dissection with repair at 52 years old (Fig. 1*B*), abdominal hernia repair at 34 years of age, and myopia. The histopathological analysis of her resected aortic tissue also showed cystic medial necrosis with a disorganized appearance of collagen and elastic lamellae (Fig. 1*C*). She underwent expanded genetic testing, which failed to reveal a causal mutation in *TGFBR1*, *TGFBR2*, *ACTA2*, *COL3A1*, *MYH11*, *SLC2A10*, *SMAD3*, or *MYLK*. A variant of unknown significance c.703G > C (p.V235L) was found in the *TGFB1* gene. Clinical features of other family members are provided in Table S1.

Identification of a Missense Mutation in *LOX* Associated with FTAAD. In November of 2013, we performed whole-genome sequencing in two first cousins with TAAD (Fig. 1*A*, individuals III-1 and III-3) to identify the causal gene and mutation underlying the disease in this family. We required putative causal mutations to (*i*) be shared in a heterozygous state between these two individuals; (*ii*) be rare, with a minor allele frequency in all populations from the National Heart Lung and Blood Institute Exome Sequencing Program and Exome Aggregation Consortium of 0.01% or less, and not be observed in a local database of individuals sequenced for other rare, nonvascular Mendelian disorders; and (*iii*) exert a functional impact on the gene's product, restricting our analysis to missense, nonsense, frameshift, or splice site variants. This analysis resulted in a total of seven candidate mutations (Table S2); six of these were eliminated because of lack of cosegregation with disease (i.e., either not present in other affected individuals from the family or present in unaffected individuals in the family) or other considerations (details are in Table S2).

The remaining candidate mutation was a missense substitution (c.893T > G encoding p.Met298Arg) (Fig. S1) in *LOX*, which was considered a strong candidate because of the gene's known role in arterial wall biology (12, 13). LOX, an enzyme that requires copper for its activity, catalyzes the cross-linking of collagen and elastin by deaminating side chains of specific lysine and hydroxylysine residues (15). Methionine at amino acid 298 is highly conserved and located within the copper binding domain of LOX (Fig. 1*D*), suggesting that this missense mutation might disrupt normal LOX function.

Mice Heterozygous for the *Lox* Missense Variant Have Longer Ascending Aortas with Fragmented Elastic Fibers. To explore the functional relevance of the *LOX* p.M298R mutation in terms of vascular disease and determine how the mutation affects LOX function, we used clustered regularly interspaced short palindromic repeats (CRISPR)/clustered regularly interspaced short palindromic repeats-associated protein-9 nuclease (Cas9) genome editing to introduce the human mutation into the homologous site in the mouse genome that corresponds to amino acid 292 (*Lox* p.M292R) (Fig. S2). Animals heterozygous for the mutation ($Lox^{+/M292R}$; hereafter referred to as $Lox^{+/Mut}$) appeared grossly normal and showed no increased mortality through 6 mo of age. Aortic diameter in $Lox^{+/Mut}$ animals was normal, but ascending aortic length measured from the aortic root to the brachiocephalic artery was 10% longer in the $Lox^{+/Mut}$ animals (3.28 ± 0.05 mm; $n = 9$) compared with $Lox^{+/+}$ littermate controls (2.94 ± 0.06 mm; $n = 7$) (Fig. 2*A*). Compared with $Lox^{+/+}$ littermate controls, the $Lox^{+/Mut}$ animals did not have significantly different systolic (110.71 ± 9.96 vs. 118.22 ± 9.46 mmHg in $Lox^{+/+}$ and $Lox^{+/Mut}$ animals, respectively; $P = 0.15$) or diastolic (75.57 ± 8.30 vs. 77.56 ± 4.19 mmHg in $Lox^{+/+}$ and $Lox^{+/Mut}$ animals, respectively; $P = 0.87$) blood pressure, although we cannot exclude the possibility of a small difference (Fig. 2*B*). Circumferential

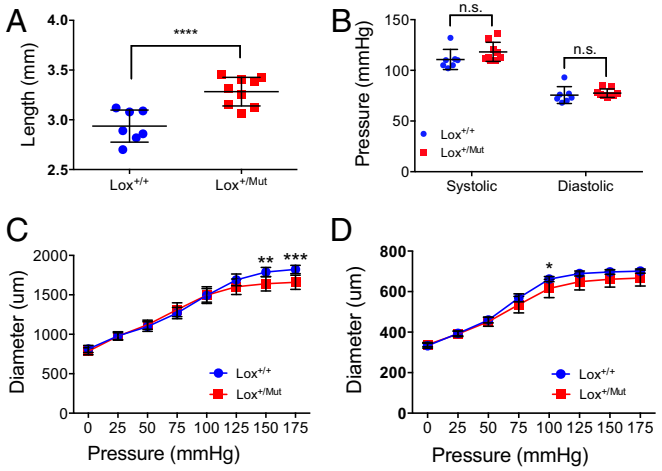

Fig. 2. $Lox^{+/Mut}$ animals have altered aortic wall dimensions and normal blood pressure. (*A*) The length of the ascending aorta from the heart to the brachiocephalic artery is significantly longer in 3-mo-old $Lox^{+/Mut}$ animals compared with $Lox^{+/+}$ littermate controls. ****$P = 0.0005$. (*B*) Blood pressure measurements using an arterial catheter found no difference in systolic ($P = 0.15$) or diastolic ($P = 0.87$) blood pressure between $Lox^{+/+}$ and $Lox^{+/Mut}$ mice. n.s., not significant. Pressure–diameter responses collected for (*C*) the left common carotid artery and (*D*) ascending aorta show that both vessels in $Lox^{+/Mut}$ animals are slightly stiffer than controls at high pressure but are not different in the physiological pressure range. Data are from $n = 9$ $Lox^{+/Mut}$ and $n = 7$ $Lox^{+/+}$ animals. *$P = 0.02$; **$P = 0.001$; ***$P = 0.0002$.

vessel wall stiffness, extrapolated from pressure/diameter measurements (Fig. 2 *C* and *D*), showed a stiffer carotid and ascending aorta at high pressures compared with in $Lox^{+/+}$ animals but normal circumferential stiffness at lower pressures. These findings indicate that the $Lox^{+/Mut}$ animals have altered vessel wall material properties but normal vessel wall mechanics at physiologic pressures.

Ultrastructural analysis of the unloaded $Lox^{+/Mut}$ aorta showed a thicker arterial wall with an appropriate number (7 to 8) of elastic lamellae and smooth muscle cell layers (Fig. 3*A*). Although there were regions of the wall that were morphologically normal, the majority of areas in the aortic tissue of $Lox^{+/Mut}$ mice had discontinuous elastic lamellae compared with the normal lamellae seen in $Lox^{+/+}$ mice (Fig. 3*A*). The abnormal lamellae observed in the aortic walls of $Lox^{+/Mut}$ mice were similar to those in $Lox^{+/-}$ mice. Autofluorescence of elastin in aortic tissue (Fig. 3*B*) showed that these breaks were present at significantly higher density throughout the aorta of $Lox^{+/Mut}$ mice compared with $Lox^{+/+}$ littermate controls (29.9 vs. 11.9 breaks per 1 mm, respectively; $P = 0.0006$).

Mice Homozygous for the *Lox* Missense Variant Die Shortly After Birth Because of Ruptured Aortic Aneurysms. Mice homozygous for the mutation ($Lox^{Mut/Mut}$) were born alive but did not survive more than a few hours. These animals were similar in size to their $Lox^{+/+}$ and $Lox^{+/Mut}$ littermates (Fig. 4*A*), although cranial, thoracic, and abdominal hemorrhages associated with internal bleeding were frequently observed (Fig. 4*B*). Some animals had severe kyphosis (Fig. 4*A*) and ruptured diaphragms. All $Lox^{Mut/Mut}$ animals had highly tortuous vessels with aneurysms in the ascending aorta and/or aortic arch as well as frequent aneurysms in the descending abdominal aorta near the renal artery branches (Fig. 4*C*).

***Lox* Missense Mutation Does Not Decrease mRNA Expression or Protein Synthesis.** Gene array analysis showed that all *Lox* family members (*Lox*, *Loxl1*, *Loxl2*, *Loxl3*, and *Loxl4*) are expressed in the developing aorta, with *Lox* having the highest expression level at every developmental time point (Fig. S3). *Loxl1* is the second most highly expressed member, with an expression pattern similar to *Lox* but at levels two- to fourfold less. Both *Lox* and *Loxl1* reach their highest expression levels during the late fetal period followed by relatively constant expression until decreasing rapidly around postnatal day 30 (P30). Expression of *Loxl3*, in contrast, is highest postnatally (P0–P21). *Loxl2* and *Loxl4* have low but detectable levels that remain relatively unchanged from the embryonic period through adulthood.

To determine if the *Lox* mutation alters expression of the mutant gene, quantitative real-time PCR was performed on mRNA from aortic tissue of newborn animals (P0). We found that *Lox* and other *Lox* isoforms were expressed in aortic tissue from $Lox^{+/Mut}$ and $Lox^{Mut/Mut}$ animals at the same levels as littermate controls (Fig. 5*A*). In addition, the mutation did not block pro-Lox protein synthesis (Fig. 5*A*, *Inset*).

***Lox* Missense Mutation Decreases Enzymatic Activity.** Given the evidence that the *Lox* mutation did not decrease gene expression or protein synthesis, we next investigated the effect of the mutation on protein function. To determine the enzymatic activity level of the mutant Lox protein, we cultured primary mouse embryonic fibroblasts (MEFs) from $Lox^{+/+}$ and $Lox^{Mut/Mut}$ animals. Lox secreted into the culture medium was collected, and enzyme activity was measured by the production of fluorescent resorufin using the Amplex Red assay at 0, 30, 60, 90, 120, and 150 min. Lox activity in MEFs cultured from $Lox^{+/+}$ animals was significantly higher than that from $Lox^{Mut/Mut}$ animals beginning at 60 min (Fig. 5*B*). There was no significant difference in Lox

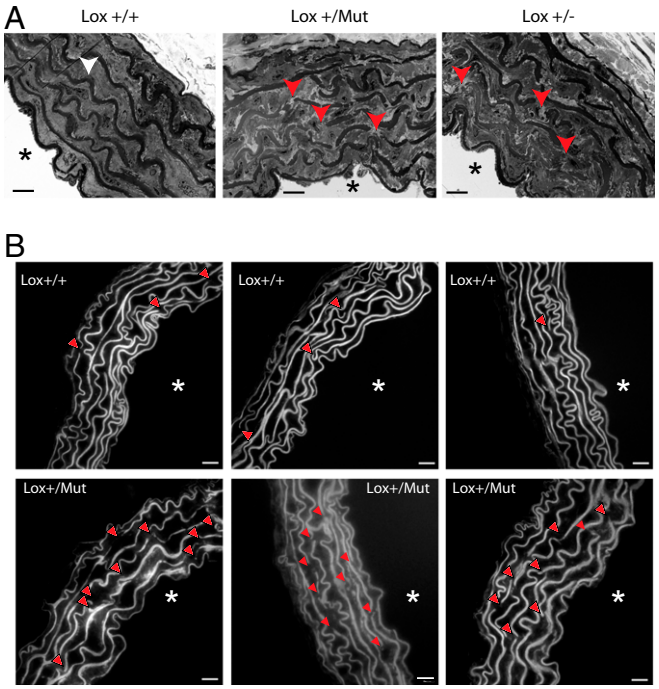

Fig. 3. $Lox^{+/Mut}$ animals have altered ultrastructural properties of the aortic wall. (*A*) EM of the ascending aorta from $Lox^{+/+}$, $Lox^{+/Mut}$, and $Lox^{+/-}$ mice. The aortic walls of $Lox^{+/+}$ animals showed smooth and continuous elastic lamellae (white arrowhead), whereas aortas from both $Lox^{+/Mut}$, and $Lox^{+/-}$ mice were found to be thicker with fragmented (red arrowheads) and disorganized elastic lamellae. (Scale bar: 10 μm.) *Aortic lumen. (*B*) Autofluorescence of elastin in aortic tissue showed that this was not an isolated finding and found that $Lox^{+/Mut}$ animals had a significantly higher density of elastic lamellae breaks (red arrowheads) compared with $Lox^{+/+}$ mice ($P = 0.0006$). (Scale bar: 20 μm.) *Aortic lumen.

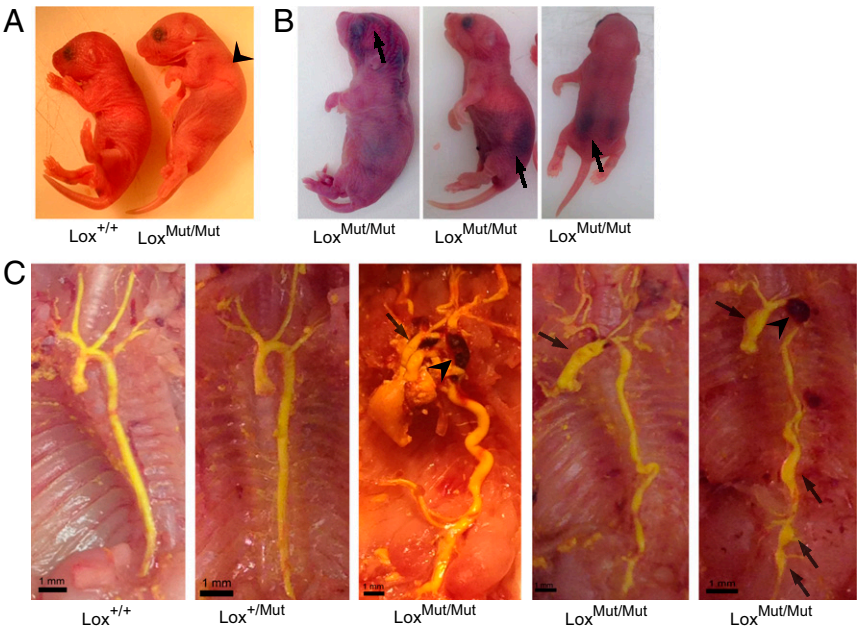

Fig. 4. $Lox^{Mut/Mut}$ exhibit normal size, kyphosis, hemorrhages, and arterial tortuosity, and they die perinatally of aortic aneurysm/dissection. (*A*) $Lox^{Mut/Mut}$ animals were born in the expected Mendelian numbers but died within a few hours of birth. Body size of the mutant animals was comparable with WT and heterozygous littermates. Some $Lox^{Mut/Mut}$ animals had severe kyphosis (arrowhead in *A*), and cranial, thoracic, and abdominal hemorrhages (arrows in *B*) were common. Arterial architecture visualized by yellow latex injection into the left ventricle showed that $Lox^{Mut/Mut}$ animals have highly tortuous vessels together with ascending and abdominal aortic aneurysms (arrows in *C*). Vessel tortuosity or aneurysms were not observed in $Lox^{+/+}$ or $Lox^{+/Mut}$ littermates. Blood clots around blood vessels (arrowheads in *C*) indicated that aneurysmal rupture was a frequent occurrence in $Lox^{Mut/Mut}$ mice. (Scale bar: 1 mm.)

activity between conditioned media from $Lox^{Mut/Mut}$ MEFs and cell-free media samples.

Discussion

Through whole-genome sequencing in two affected individuals from a family exhibiting autosomal dominant TAAD, we identified a missense mutation in the copper binding region of *LOX* as the most likely causal variant. To further evaluate the significance and potential impact of this variant, we used genome engineering techniques to insert the human mutation into the orthologous position in the mouse genome. Mice bred to homozygosity for the human mutation recapitulated the human phenotype, supporting the likely causal role of this mutation in the human disease. This conclusion is further bolstered by the recent identification of additional FTAAD probands harboring *LOX* mutations (16).

Several conclusions emerge from our results. First, we report another successful use of genome-scale sequencing in mapping a causal gene underlying human disease. With the advent of next generation DNA sequencing technology (17), the cost and time of genome-scale sequencing have both decreased substantially. In small kindreds, such as the one presented in this study—in which the traditional mapping tools of linkage and directed sequencing are unlikely to provide a definitive result—genome-scale (either whole-exome or whole-genome) sequencing provides a rapid and cost-effective alternative means of identifying the causal variant and gene (18).

Second, although the historically accepted criteria for considering a novel gene causal in Mendelian disease include identifying additional kindreds with the same phenotype harboring independent variants in the same gene (19), these standards are likely to be increasingly difficult to meet in the future. After sequencing 410 unrelated FTAAD probands, Guo et al. (16) identified five possibly causal mutations in *LOX*, suggesting that this gene is probably responsible for ≤1% of FTAAD. As gene mapping studies continue to identify novel genes underlying FTAAD and other Mendelian diseases, new gene discoveries will invariably represent increasingly smaller proportions of the inherited basis of disease. Thus, new techniques and criteria for proving causality in Mendelian disease should be considered. Genome engineering techniques in animal models to study the in vivo effects of human alleles represent one path forward in the absence of identifying additional humans with disease.

Third, the generation of an animal model specific to this genetic defect provides insight into the potential mechanism underlying the disease. LOX is the major ECM cross-linking enzyme in blood vessels, and loss of Lox activity through either enzyme inhibition or gene inactivation leads to vascular dilatation and rupture (12, 13). Although mutations in *LOX* had not hitherto been associated with human disease, alterations in LOX expression levels and functional activity have been observed in diverse genetic disorders, with some having vascular involvement. For example, reduced LOX activity has been reported in two X-linked recessively inherited disorders, Menkes disease and occipital horn syndrome (20), which are caused by mutations in the *ATP7A* gene encoding a copper-transporting ATPase. Moreover, mottled blotchy mice, which carry mutations in *Atp7a*, also have high incidence of aortic aneurysms and exhibit disrupted elastic fibers (21). Functional inhibition of Lox by the toxin β-aminoproprionitrile, which is present at high levels in peas and lentils, has been shown to cause osteolathyrism (22), a connective tissue disease characterized by skeletal abnormalities and aortic dissections. The vascular phenotype of the mutant mice, including fragmented elastic lamellae in $Lox^{+/Mut}$ animals and tortuous and aneurysmal vessels in animals homozygous for the mutation, resembles vascular changes seen in *Lox* KO animals (12, 13), implying that the arginine for methionine substitution leads to loss of Lox function. In fact, we identified similar abnormalities of the aortic wall architecture in both $Lox^{+/Mut}$ and $Lox^{+/-}$ mice, suggesting that the p.M298R missense change results in a functionally null enzyme. This conclusion was further corroborated by the observation that fibroblasts derived from $Lox^{Mut/Mut}$ animals did not secrete Lox with enzymatic activity that was detectable above baseline. While this result is in contrast to a recent study suggesting that FTAAD was associated with missense mutations in *LOX* which only partially decreased protein function (16), methodological differences may account for this discrepancy. For example, our assay tested the function of Lox that was secreted from cells that were only producing mutant protein, whereas the other study tested the function of LOX present in the cell lysates of cultured human cells (which express normal LOX) that were overexpressing the mutant protein.

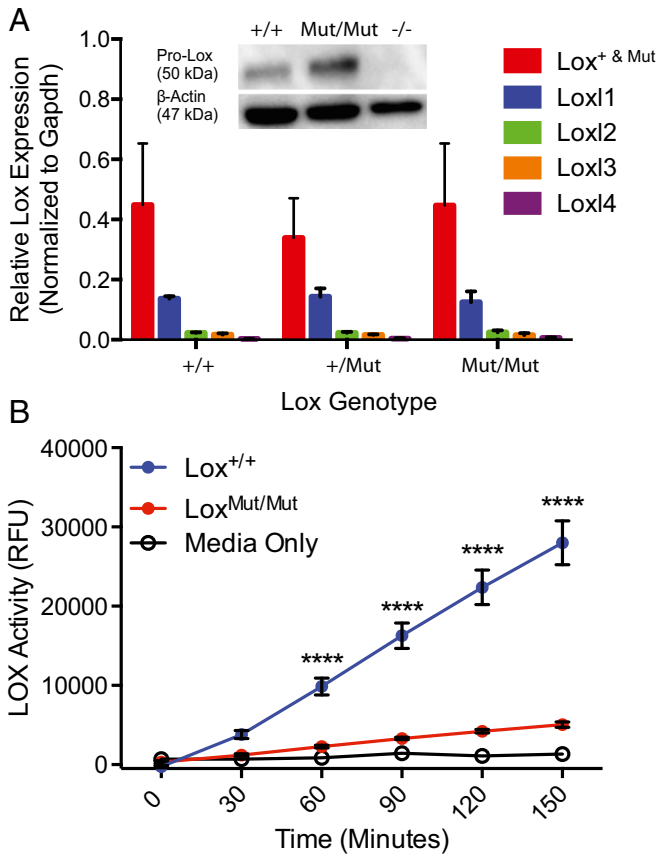

Fig. 5. Mutant Lox is expressed and synthesized but lacks enzymatic activity. (*A*) Quantitative RT-PCR analysis of mRNA from the aortas of $Lox^{+/+}$, $Lox^{+/Mut}$, and $Lox^{Mut/Mut}$ P0 animals showed normal expression levels of all Lox family members in all three genotypes (note that the *Lox* primer/probe recognizes both Lox^{+} and Lox^{Mut} alleles). Two-way ANOVA $P = 0.63$ for $Lox^{+/+}$ vs. $Lox^{+/Mut}$; $P = 0.99$ for $Lox^{+/+}$ vs. $Lox^{Mut/Mut}$; and $P = 0.63$ for $Lox^{+/Mut}$ vs. $Lox^{Mut/Mut}$. (*Inset*) Lox protein immunoblotting confirmed that the mutant Lox protein is produced by $Lox^{Mut/Mut}$ cells at levels similar to the WT ($Lox^{+/+}$) protein. The absence of a band in extracts of $Lox^{-/-}$ cells confirms the specificity of the Lox antibody. (*B*) Lox activity in the presence and absence of β-aminopropionitrile (BAPN) was assayed in conditioned culture medium from $Lox^{+/+}$ and $Lox^{Mut/Mut}$ MEFs at 30-min time intervals. Medium incubated without cells served as the baseline control. MEFs cultured from two $Lox^{+/+}$ and three $Lox^{Mut/Mut}$ embryos were tested in duplicates for $n = 4$ and $n = 6$, respectively, and plotted according to genotype at each time point (mean ± SEM). Lox activity, which is the difference between activity with and without BAPN, is expressed in relative fluorescent units (RFUs). $^{****}P < 0.0001$.

There are several mechanisms by which the missense change that we studied may result in loss of function. The introduction of an arginine residue within the copper binding domain may reduce the ability of the enzyme to bind copper, leading to loss of catalytic activity. Alternatively, it might disrupt normal LOX protein processing, or it could produce a dominant negative effect from decreased substrate binding. It is also possible that the mutant LOX protein is unable to interact with fibulin-4 (23) or components of the TGF-β signaling pathway (24)—both of which are known functions of LOX—thereby leading to aortic disease. It should be noted that, although *Loxl1* is expressed at appreciably high levels in the aorta, it cannot compensate for loss of Lox activity and that mice lacking *Loxl1* do not have a vascular phenotype (25). Future studies will be needed to clarify the exact mechanism by which this mutation leads to loss of Lox function.

Similar to other genetically engineered mouse models of human aortic disease (26, 27), we did not observe any aneurysm or other arterial disease in $Lox^{+/Mut}$ mice. There are many reasons why the severity of phenotypes observed in murine models might differ from that seen in humans (28), and for reasons that are not completely understood, mutations causing human disease in an autosomal dominant manner often reproduce disease in mouse models only when present in a homozygous state (29). Despite the lack of overt disease in the heterozygous mouse, however, the increased ascending aortic length and fragmented elastic fibers in $Lox^{+/Mut}$ mice suggest that mutant animals may be predisposed to vascular diseases because of weakened vessel walls under stress conditions. This reasoning may explain why some individuals in the family (for example, individual II-3) do not appear to develop aneurysm or dissection and are only affected with arterial tortuosity (Fig. S4). Additional studies in which heterozygous mice are subjected to hemodynamic stress conditions may provide additional insight into this question.

Finally, our genome engineering approach has created a framework in which therapeutic hypotheses relevant to this genetic form of disease may be directly tested. For example, the observations that LOX activity is directly correlated with dietary copper and increases even when dietary copper supplementation is above what is needed for normal growth and development (30, 31) promote the hypothesis that copper supplementation in humans with TAAD caused by *LOX* mutations might augment the LOX enzymatic function of the normal allele and prevent vascular disease (although this approach is complicated by the fact that supplementation would need to be initiated early in embryonic development before a genetic diagnosis could easily be made). Regardless, hypotheses such as this are now directly testable using our mouse model of the human mutation. More generally, beyond individuals with TAAD caused by *LOX* mutations, there is evidence that LOX may also play a role in modifying other forms of TAAD (32–34), which suggests that therapeutic manipulation of LOX activity may prove beneficial in other inherited aortopathies.

In summary, the discovery of *LOX* mutations underlying TAAD in this family and others (16) suggests that this gene plays an important role in disease. Sequencing this gene may be useful in identifying the genetic basis for additional FTAAD probands and families. Future mouse model system studies of *Lox* mutations may provide additional mechanistic insights into disease pathogenesis and potential therapeutic options specific to this genetic cause.

Methods

Family Recruitment and Genome Sequencing. The family examined in this study was referred to our clinic because of the two-generational history of aortic dissection. Eight members of the family were recruited for the study (Fig. 1*A* and Table S1). The Partners Healthcare Institutional Review Board approved the human research portion of the study, and informed consent was obtained from all study participants. Individuals I-2, II-1, II-2, II-3, III-1, and III-2 (Fig. 1*A* and Table S1) were examined in our clinic. Individuals III-3 and III-4 were evaluated at another hospital, and their records were subsequently reviewed. Whole-genome sequencing was performed by the Illumina Clinical Services Laboratory (Illumina, Inc.) as described in *SI Methods*.

Generation of Animals Harboring the *Lox* Mutation. CRISPR/Cas9 genome editing technology was used in collaboration with the Washington University School of Medicine Hope Center Transgenic Vectors Core to generate mice harboring the *Lox* mutation identified in our family at the homologous murine position (c.857T > G encoding p.M292R) as detailed in *SI Methods*. All animal studies were performed according to protocols approved by the Animal Studies Committee of the Washington University School of Medicine.

Blood Pressure and Vessel Mechanical Property Measurements. Blood pressure, ascending aortic length, and compliance of the ascending aorta and left common carotid arteries were measured in $Lox^{+/+}$ ($n = 7$) and $Lox^{+/Mut}$ ($n = 9$) animals at 3 mo of age as described in *SI Methods*. The differences in ascending aortic length and blood pressure between $Lox^{+/+}$ and $Lox^{+/Mut}$

animals were assessed using a *t* test. The difference in compliance between $Lox^{+/+}$ and $Lox^{+/Mut}$ animals was tested using a two-way ANOVA.

Internal Aortic Latex Casting. Because animals homozygous for the missense mutation ($Lox^{Mut/Mut}$) die shortly after birth, newborn (P0) pups from $Lox^{+/Mut} \times Lox^{+/Mut}$ breeders were used to visualize the vascular architecture of $Lox^{+/+}$ ($n = 7$), $Lox^{+/Mut}$ ($n = 24$), and $Lox^{Mut/Mut}$ ($n = 5$) animals. After euthanasia, PBS was flushed through the left ventricle of the heart followed by injection of 200 μL yellow latex diluted in deionized water in a 1:1 ratio. The latex was allowed to polymerize at 4 °C for 3 h before fixing the entire animals in 10% (vol/vol) buffered formalin overnight at 4 °C. The formalin was replaced with 70% (vol/vol) ethanol 2 h before dissection.

Quantification of *Lox* mRNA Levels. Aorta and lung tissue were collected from $Lox^{+/+}$ ($n = 3$), $Lox^{+/Mut}$ ($n = 3$), and $Lox^{Mut/Mut}$ ($n = 4$) P0 animals and stored in RNAlater Solution (ThermoFisher Scientific) at −20 °C. Total RNA was collected using TRIzol (ThermoFisher Scientific) following the manufacturer's protocol, and real-time PCR was performed using techniques described in *SI Methods*.

MEF Culturing, Immunoblotting, and Lox Activity Assay. Primary MEF cultures were established from embryonic day 14.5 embryos harvested from $Lox^{+/Mut} \times Lox^{+/Mut}$ breeders as previously described (35) and maintained as described in *SI Methods*. Lox protein immunoblotting and enzymatic activity were performed as described in *SI Methods*.

Ultrastructural Analysis and Elastin Fluorescence Imaging of the Aortic Wall. For EM, aortas from 3-mo-old $Lox^{+/+}$ ($n = 3$), $Lox^{+/Mut}$ ($n = 3$), and $Lox^{-/-}$ ($n = 3$) animals were prepared and imaged as described in *SI Methods*. To visualize elastin lamellae in the aortic wall, the ascending aortas from 3-mo-old $Lox^{+/Mut}$ ($n = 3$) mice and their $Lox^{+/+}$ ($n = 3$) WT littermate controls were prepared and imaged as described in *SI Methods*. The difference in the number of breaks per millimeter between $Lox^{+/+}$ and $Lox^{+/Mut}$ animals was assessed using a *t* test.

ACKNOWLEDGMENTS. We thank the family presented here for participating in this study. We also thank Russell Knutsen and Marilyn Levy for the mouse physiology and EM studies, respectively; and Phillip Trackman (Boston University) for assistance with the LOX activity assay. This work was supported, in part, by the Hope Center Transgenic Vectors Core and Mouse Genetics Core at the Washington University School of Medicine. Funds supporting this work were provided by National Heart, Lung, and Blood Institute Grants R01HL105314 (to R.P.M.), R01HL53325 (to R.P.M.), K08HL114642 (to N.O.S.), and R01HL131961 (to N.O.S.). V.S.L. was supported by National Institute of Biomedical Imaging and Bioengineering Training Grant T32EB18266 and National Heart, Lung, and Blood Institute Training Grant T32HL125241. C.M.H. is a Scholar of the Child Health Research Center at Washington University School of Medicine (K12-HD076224). R.P.M. and N.O.S. are also supported, in part, by The Foundation for Barnes-Jewish Hospital.

1. Guo DC, et al. (2007) Mutations in smooth muscle alpha-actin (ACTA2) lead to thoracic aortic aneurysms and dissections. *Nat Genet* 39(12):1488–1493.
2. Lee B, et al. (1991) Linkage of Marfan syndrome and a phenotypically related disorder to two different fibrillin genes. *Nature* 352(6333):330–334.
3. Loeys BL, et al. (2005) A syndrome of altered cardiovascular, craniofacial, neurocognitive and skeletal development caused by mutations in TGFBR1 or TGFBR2. *Nat Genet* 37(3):275–281.
4. Loeys BL, et al. (2006) Aneurysm syndromes caused by mutations in the TGF-beta receptor. *N Engl J Med* 355(8):788–798.
5. Tsipouras P, et al. (1986) Ehlers-Danlos syndrome type IV: Cosegregation of the phenotype to a COL3A1 allele of type III procollagen. *Hum Genet* 74(1):41–46.
6. van de Laar IM, et al. (2011) Mutations in SMAD3 cause a syndromic form of aortic aneurysms and dissections with early-onset osteoarthritis. *Nat Genet* 43(2):121–126.
7. Wang L, et al. (2010) Mutations in myosin light chain kinase cause familial aortic dissections. *Am J Hum Genet* 87(5):701–707.
8. Zhu L, et al. (2006) Mutations in myosin heavy chain 11 cause a syndrome associating thoracic aortic aneurysm/aortic dissection and patent ductus arteriosus. *Nat Genet* 38(3):343–349.
9. Guo DC, et al. (2013) Recurrent gain-of-function mutation in PRKG1 causes thoracic aortic aneurysms and acute aortic dissections. *Am J Hum Genet* 93(2):398–404.
10. Coucke PJ, et al. (2006) Mutations in the facilitative glucose transporter GLUT10 alter angiogenesis and cause arterial tortuosity syndrome. *Nat Genet* 38(4):452–457.
11. Smith-Mungo LI, Kagan HM (1998) Lysyl oxidase: Properties, regulation and multiple functions in biology. *Matrix Biol* 16(7):387–398.
12. Mäki JM, et al. (2002) Inactivation of the lysyl oxidase gene Lox leads to aortic aneurysms, cardiovascular dysfunction, and perinatal death in mice. *Circulation* 106(19): 2503–2509.
13. Hornstra IK, et al. (2003) Lysyl oxidase is required for vascular and diaphragmatic development in mice. *J Biol Chem* 278(16):14387–14393.
14. Lopez KM, Greenaway FT (2011) Identification of the copper-binding ligands of lysyl oxidase. *J Neural Transm (Vienna)* 118(7):1101–1109.
15. Eyre DR, Paz MA, Gallop PM (1984) Cross-linking in collagen and elastin. *Annu Rev Biochem* 53:717–748.
16. Guo DC, et al. (2016) LOX mutations predispose to thoracic aortic aneurysms and dissections. *Circ Res* 118(6):928–934.
17. Shendure J, Ji H (2008) Next-generation DNA sequencing. *Nat Biotechnol* 26(10): 1135–1145.
18. Bamshad MJ, et al. (2011) Exome sequencing as a tool for Mendelian disease gene discovery. *Nat Rev Genet* 12(11):745–755.
19. MacRae CA (2012) Action and the actionability in exome variation. *Circ Cardiovasc Genet* 5(6):597–598.
20. Lazoff SG, Rybak JJ, Parker BR, Luzzatti L (1975) Skeletal dysplasia, occipital horns, diarrhea and obstructive uropathy- a new hereditary syndrome. *Birth Defects Orig Artic Ser* 11(5):71–74.
21. Andrews EJ, White WJ, Bullock LP (1975) Spontaneous aortic aneurysms in blotchy mice. *Am J Pathol* 78(2):199–210.
22. Norton TB, Dasler W, Milliser RV (1965) Osteolathyrism in the hamster: Pathological and chemical changes produced by beta-aminopropionitrile in connective tissues. *Proc Soc Exp Biol Med* 118:90–94.
23. Horiguchi M, et al. (2009) Fibulin-4 conducts proper elastogenesis via interaction with cross-linking enzyme lysyl oxidase. *Proc Natl Acad Sci USA* 106(45): 19029–19034.
24. Atsawasuwan P, et al. (2008) Lysyl oxidase binds transforming growth factor-beta and regulates its signaling via amine oxidase activity. *J Biol Chem* 283(49):34229–34240.
25. Liu X, et al. (2004) Elastic fiber homeostasis requires lysyl oxidase-like 1 protein. *Nat Genet* 36(2):178–182.
26. Judge DP, et al. (2004) Evidence for a critical contribution of haploinsufficiency in the complex pathogenesis of Marfan syndrome. *J Clin Invest* 114(2):172–181.
27. Pereira L, et al. (1997) Targetting of the gene encoding fibrillin-1 recapitulates the vascular aspect of Marfan syndrome. *Nat Genet* 17(2):218–222.
28. Libby P (2015) Murine "model" monotheism: An iconoclast at the altar of mouse. *Circ Res* 117(11):921–925.
29. Seidman JG, Seidman C (2002) Transcription factor haploinsufficiency: When half a loaf is not enough. *J Clin Invest* 109(4):451–455.
30. Rucker RB, et al. (1998) Copper, lysyl oxidase, and extracellular matrix protein cross-linking. *Am J Clin Nutr* 67(5 Suppl):996S–1002S.
31. Opsahl W, et al. (1982) Role of copper in collagen cross-linking and its influence on selected mechanical properties of chick bone and tendon. *J Nutr* 112(4):708–716.
32. Busnadiego O, et al. (2015) Elevated expression levels of lysyl oxidases protect against aortic aneurysm progression in Marfan syndrome. *J Mol Cell Cardiol* 85:48–57.
33. Choudhary B, et al. (2009) Absence of TGFbeta signaling in embryonic vascular smooth muscle leads to reduced lysyl oxidase expression, impaired elastogenesis, and aneurysm. *Genesis* 47(2):115–121.
34. Oleggini R, Gastaldo N, Di Donato A (2007) Regulation of elastin promoter by lysyl oxidase and growth factors: Cross control of lysyl oxidase on TGF-beta1 effects. *Matrix Biol* 26(6):494–505.
35. Jain K, Verma PJ, Liu J (2014) Isolation and handling of mouse embryonic fibroblasts. *Methods Mol Biol* 1194:247–252.
36. Li H, Durbin R (2009) Fast and accurate short read alignment with Burrows-Wheeler transform. *Bioinformatics* 25(14):1754–1760.
37. DePristo MA, et al. (2011) A framework for variation discovery and genotyping using next-generation DNA sequencing data. *Nat Genet* 43(5):491–498.
38. McLaren W, et al. (2010) Deriving the consequences of genomic variants with the Ensembl API and SNP Effect Predictor. *Bioinformatics* 26(16):2069–2070.
39. Faury G, et al. (2003) Developmental adaptation of the mouse cardiovascular system to elastin haploinsufficiency. *J Clin Invest* 112(9):1419–1428.
40. Dell RB, Holleran S, Ramakrishnan R (2002) Sample size determination. *ILAR J* 43(4): 207–213.
41. Thomassin L, et al. (2005) The Pro-regions of lysyl oxidase and lysyl oxidase-like 1 are required for deposition onto elastic fibers. *J Biol Chem* 280(52):42848–42855.
42. Hurtado PA, et al. (2008) Lysyl oxidase propeptide inhibits smooth muscle cell signaling and proliferation. *Biochem Biophys Res Commun* 366(1):156–161.
43. Palamakumbura AH, Trackman PC (2002) A fluorometric assay for detection of lysyl oxidase enzyme activity in biological samples. *Anal Biochem* 300(2):245–251.
44. McLean S, Mecham B, Kelleher C, Mariani T, Mecham R (2005) Extracellular matrix gene expression in developing mouse aorta. *Extracellular Matrices and Development*, ed Miner J (Elsevier, New York), pp 82–128.
45. Pelletier S, Gingras S, Howell S, Vogel P, Ihle JN (2012) An early onset progressive motor neuron disorder in Scyl1-deficient mice is associated with mislocalization of TDP-43. *J Neurosci* 32(47):16560–16573.
46. Terenzio M, et al. (2014) Bicaudal-D1 regulates the intracellular sorting and signalling of neurotrophin receptors. *EMBO J* 33(14):1582–1598.
47. Wang Y, et al. (2008) MUC16 expression during embryogenesis, in adult tissues, and ovarian cancer in the mouse. *Differentiation* 76(10):1081–1092.